

EREM 77/4

Journal of Environmental Research,
Engineering and Management
Vol. 77 / No. 4 / 2021
pp. 99–121
DOI 10.5755/j01.erem.77.4.29560

Investigation of Groundwater Potential Using Remote Sensing and Hydro-geophysical Techniques: A Case Study of the Telidjene Basin (Eastern Algeria)

Received 2021/08

Accepted after revision 2021/11

<http://dx.doi.org/10.5755/j01.erem.77.4.29560>

Investigation of Groundwater Potential Using Remote Sensing and Hydro-geophysical Techniques: A Case Study of the Telidjene Basin (Eastern Algeria)

Amel Hibi*, Layachi Gouaidia, Omar Guefaifia

Laboratoire Environnement Sédimentaire, Ressources Minérales et Hydriques de l'Algérie Orientale, Département des Sciences de la Terre, Université Larbi Tebessi, Route de Constantine, 12002, Tébessa, Algérie

*Corresponding author: amel.hibi@univ-tebessa.dz

The present study aims to assess groundwater potential in the Telidjene Basin located in the semi-arid part of eastern Algeria, applying an innovative approach combining both remote sensing and hydrogeophysics methods. A re-interpretation of geophysical data and vertical electrical sounding (VES) measurements were applied and calibrated with the borehole data to map the deep structures that may control the presence of groundwater and identify the geological and hydrogeological setting. Morphometric factors affecting recharge were mapped using several types of remote sensing data (SRTM DEM, Landsat-8). Thematic maps were overlaid using the multicriteria method and GIS to detect potential recharge areas. The results show that the main factors influencing recharge are fracturing and drainage density. Four potential recharge areas were identified over a 547 km² area of the basin. 20% of the area falls in the weakest class, 32% in the weak class, 3% in the moderate, and 16% in the strongest. Furthermore, the study reveals that an alluvial aquifer with a thickness of up to 60m, spreading over the surface, along the Wadi Telijene and the alluvial soil, is deposited unconformably on Cretaceous terrain containing aquifer horizons of varying thickness and different electrical resistivities (10–150

Ωm), drawing an anticlinal structure with lithostratigraphy interrupted by a series of faults and spurs of Aptian and Triassic age. The south-western part of the basin has a high to moderate recharge and storage capacity. Its alluvial cover is directly fed by precipitation and fractured limestones deposited in a syncline outcropping on the edges forming an alluvial and carbonate bilayer aquifer. This study concluded that an integrated approach, involving recent, efficient, and inexpensive technology, such as remote sensing and conventional geophysical method, can be successfully used to identify groundwater potential in the study area.

Keywords: remote sensing and GIS, groundwater potentiality, geophysics, Telidjene basin, Algeria

Introduction

In recent decades, the economic and social development of the municipalities of the Cheria district, which includes the study area, has generated a strong and growing demand for water. In addition, intense agricultural activities have put pressure on various water resources. This overexploitation, in addition to climatic hazards (semi-arid climate), has led to a significant drop in the piezometric levels of the Maastricht and Eocene aquifers. The exploration of other resources is necessary, and the aquifers of the Telidjene Basin constitute potential resources and deserve to be the subject of a more detailed and in-depth study. Thus, a good knowledge of the characteristics of the aquifers of this basin is necessary to better exploit them and preserve them from contamination.

The infrastructures, carried out by the Directorate of Water Resources since the early 1980s, have been insufficient to meet the needs of potable water and irrigation in the region under study. Thus, the lack of hydrogeological studies to examine the existing geoelectric data has led to many problems in the implementation of these infrastructures.

Previous studies conducted on the adjacent basin of Cheria (Baali, 2007) and the aquifer of "Meskina" (Gouaidia, 2008), an "anticline" with a hydraulic structure similar to that of the studied basin; have reported the influence of the geological structure on the conditions of recharge of aquifers and storage of groundwater. Baali, in his thesis on the area of Cheria located at 10 km, estimates that the average rainfall is 200 mm/year. All research conducted in the similar semi-arid context reveals that, except in karstic environments, infiltration is minimal or negligible, constituting only a supplement. In this dry climatic

context, there is a need to understand and improve the knowledge concerning the conditions of recharge and storage processes and define the influence of factors controlling them, namely, the morphometric characteristics and hydrogeological structure of aquifers in the basin.

The main objectives of this study are to assess the water resource and to improve the knowledge of the aquifer system in the Telidjene Basin using a new efficient, rapid, and low-cost approach to assist the local authorities in decision making and development planning.

To meet these objectives, the present study gives particular importance to the available data and documentation concerning the geophysical campaign (electrical soundings) (CGG, 1976) carried out in the region which has not been exploited in research yet, nor been a subject of study to any hydrogeological synthesis at the Telidjene Basin level. The study also required the execution of (7) VES in the south-western part of the basin where resources are constant, compared with the central and north-eastern part of the basin. Remote sensing data were readily available and of major use to complete the processing and produce a reliable result.

In doing so, two methods were combined: remote sensing and geophysics.

Remote sensing. Applications of remote sensing and GIS for the exploration of potential groundwater areas have been carried out by several studies in different worldwide (Krishnamurthy et al., 1996; Shaban et al., 2006; Haouchine et al., 2010; Chowdary et al., 2009; Oularé et al., 2017; Arulbalaji et al., 2019; Vasileva,

2019; Gonçalves et al., 2019), and it has been found that the factors involved in the determination of potential groundwater areas are different, and therefore the results vary accordingly. The derived results are considered satisfactory based on the field investigations and vary from region to region due to the varied geo-environmental conditions.

Geophysics. Because remote sensing data are relevant to the hydro-morphometric characteristics of the aquifer, it is necessary to incorporate other data sources such as geophysics, especially the electrical method. The use of geophysical methods provides valuable information to identify the nature as well as the geometry of the valuable information and to monitor the hydrogeological process (Zitouni et al., 2017; Moreira et al., 2021; Breusse, 1963)

This integrated methodology, combining remote sensing and geophysics, has been used by several authors and studies worldwide (Gyeltshen et al., 2020; Mohamaden et al., 2017; Ogungbade et al., 2021; Nicaise et al., 2019; Mogaji and Omobude, 2017); moreover, the new technology based on remote sensing is considered as an effective, fast and less costly tool that provides data on factors controlling the presence and water movement.

This study would be a reliable reference to help decision-makers establish their future development plans, recalling that the commune of Telidjene is counted among the most unfavorable communes and has not benefited from any budget allocated for water search actions since the 1970s.

However, the available data do not allow the evaluation of the hydrodynamic characteristics of the existing aquifers nor their geometry in-depth, which does not allow integrating them in the management tools of the water resource that require precise quantitative results.

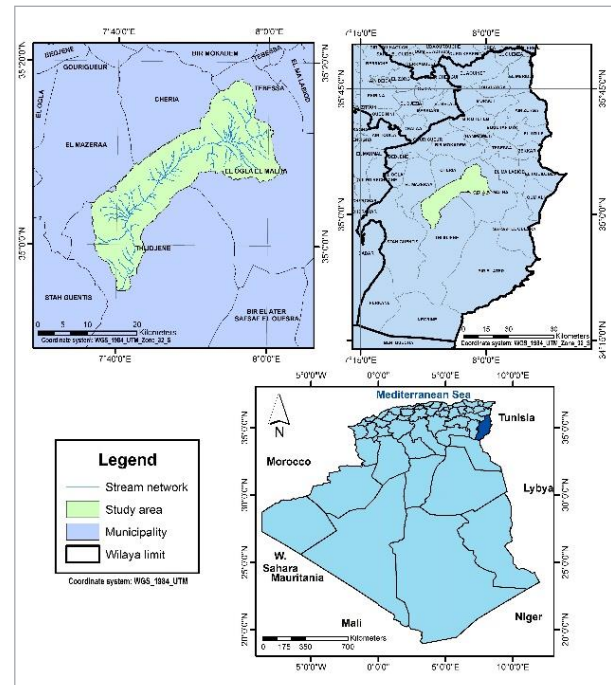
Materials and Methods

Study area

This study focuses on the Telidjene Basin, which is geographically located at the eastern end of the Saharan Atlas with an area of 547 km². Administratively,

it belongs to the commune of Telidjene, located about 70 km south-west of the wilaya of Tébessa (Fig. 1). The region is located in the topographic map of Telidjene and the map of Cheria at 1/50.000, a part of the sheet of Bir Sbeikia.

Fig. 1. Location of the study area



The Telidjene Basin (Fig. 2) is an anticline in the atlas direction (NE-SW).

The region is characterized by a semi-arid climate with a relatively cold and rainy winter and a very hot and dry summer.

Geology and hydrogeology

The basin of Telidjene is located in the south of Tébessa district, and corresponds to an anticline structure limited in the north by the reliefs of Djebel Bou Kammech, in the north-east by Djebel Krime, in the south by Djebels Debibir and Ouassif, and in the west by Djebel Aghour el Kifene (Fig. 3). The lithologic units in the study area are dominated by Tertiary, and Quaternary soils were filled during this period by sediments of continental facies from the limestone massifs that limited it. Indeed, the Wadi Telidjene and its tributaries,

draining this basin from north-east to south-west, have deposited fill material such as alluvium-forming fluvial terraces that are well developed over the entire basin, where they record very accurately the erosion activity near the NW and SO offsets (Vila, 1994a).

Fig. 2. Watershed map of the Telidjene Basin

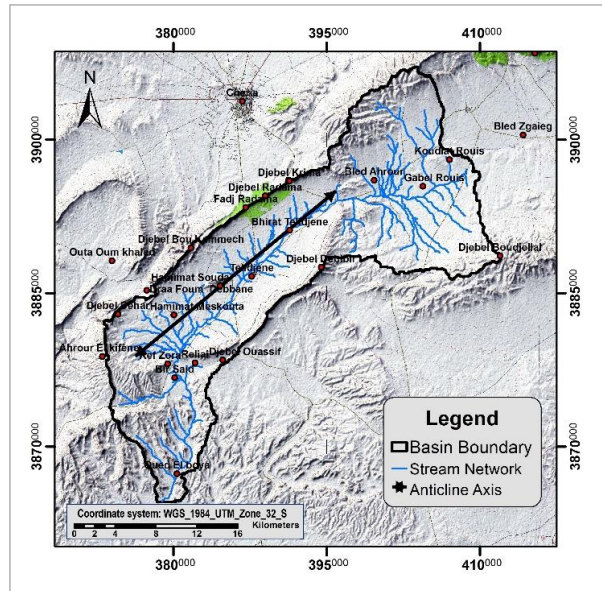
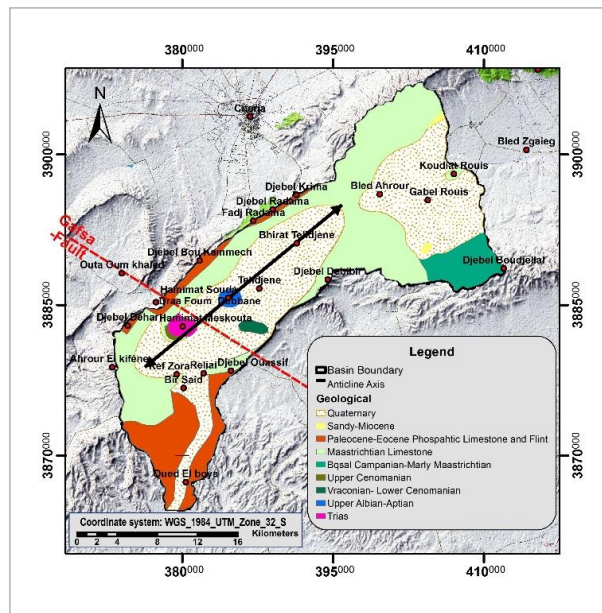


Fig. 3. Schematic geological map of the Telidjene Basin



Available lithologic logs of wells drilled in the study area indicate the coexistence of two types of aquifers, namely, superficial alluvial deposits and 'deep tertiary formations underlying the alluvial deposits,' which could have a hydraulic potential more favorable to exploitation.

The alluvial aquifer reaches a maximum of 60 m and disappears at the edges of the basin, while the carbonate aquifers could be exploited at varying depths and their thickness depending on their location in the basin and the geological structure.

As the basin is located in the atlasic domain, its structure is dominated by a vast atlasic fold with a diapiric core (Dubourdieu, 1950). This has caused several faults, giving rise to strong fracturing of the Cretaceous edge formations, which would facilitate water infiltration.

Materials

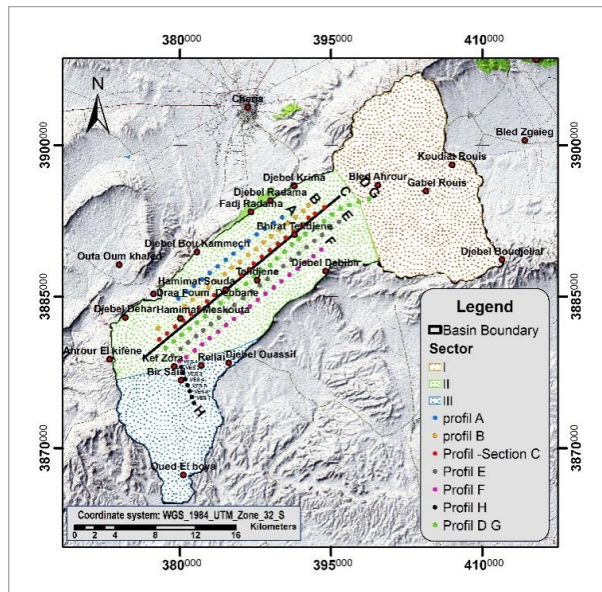
For this study, a multi-spectral image from the Landsat 8 satellite and a digital elevation model extracted from the SRTM 30 were used to extract the lineaments using the QGIS and GEOMATICA programs. The DEM digital elevation model was used to produce the thematic maps used in this work, except for the land use map, which was digitized from the map produced by the Bureau National des Etudes pour le Développement Rural (INSID, 2011). In addition, geological maps (ENERGOPROJECT-ENHYD, 2002; Vila, 1994a; Vila, 1997), at scales of 1/200 000 and 1/50 000 were processed. Geo-electrical sections of the Compagnie Générale de Géophysique (CGG, 1976) were used to produce geological and hydrogeological sections, and geological and hydrogeological data of wells and boreholes with information on geology, static water levels, flow rates, and deep lithology were used. This information was provided by the Directorate of Water Resources (DRE) and Agricultural Services (DSA) of the Tébessa district, the National Office of Geological Research (ORGM), and the National Company for Research, Production, Transport, Processing, and Marketing of Hydrocarbons (SONATRACH). Finally, with a field GPS, the coordinates of the wells were recorded with water level measurements using a manual piezometric probe (capacitive sound). Geoelectrical data were collected with an ABEM TERRAMETER SAS 300 instrument using the Schlumberger disposition.

Methods

Hydrogeophysics. To understand the geology of the catchment area, it was divided according to the morphostructural aspect into three sectors (Fig. 4).

Sector I constitutes a plain bordered by a mountainous framework formed by the Djebel Doukkane and Boudjellal, from where the rocky outcrops sometimes disturb the Mio-Plio-Quaternary cover, in particular Gabel Rouis.

Fig. 4. Map location of the geophysical profiles



Sector II is the region of the eroded dome where the reliefs are organized around an anticline ridge, locally

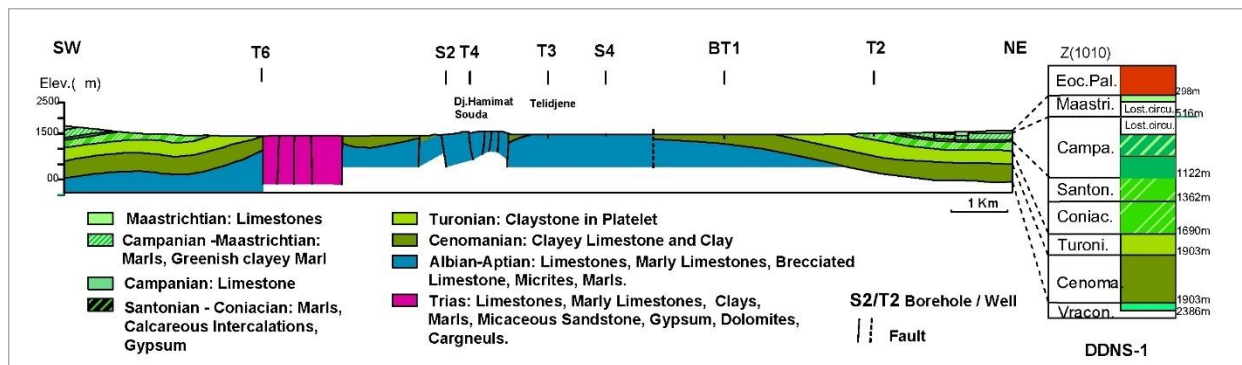
deduplicated, which is closed in the north-east by Djebel Boudjellal and Djebel Doukkane, and the south-west by Djebel Dehar and Ahrou el Kifène. The vast plain of Ain Telidjene limited by this ridge and drained to the south by the Wadi Telidjene is rugged by two derived mountains: in the west, the Hamimat-Meskouta mainly consisting of Triassic formations, and in the east, the Hamimat Souda formed of Aptian limestone. This is the region where the erosion has been the strongest and almost all the Maastrichtian and Campanian have been eroded and only appear in the summits.

Sector III is an area of subtabular fractured limestone plateaus with the typical bare landscape of the Nememcha (Vila, 1994b), which opens up to the north from the outskirts of Reliai and Kef Zora, where the limestone plunges from 50° to 30° toward the center of the basin and closes in the south.

Structure of the Telidjene Basin. A geoelectrical section (CGG, 1976, pl. 5, profile C) that passes the axis of the anticline and the Hamimat Souda spur, made on the electrical profile C (Fig. 4), totaling 20 vertical electrical soundings in AB 2000 was reinterpreted. Stratigraphic logs from different sources (Table 1) were used to calibrate the superficial horizons, whereas the DDN-101 and Bdj-2 oil drillings were used to correlate the deeper formations highlighted by the CGG geophysical survey.

The geological section (Fig. 5) shows that the anticline structure is occupied by formations ranging in age from the Maastrichtian to the Triassic (older formation), which is in abnormal contact with younger formations. The geological formations of the Telidjene

Fig. 5. Geological section through the anticline (CGG, 1976) modified



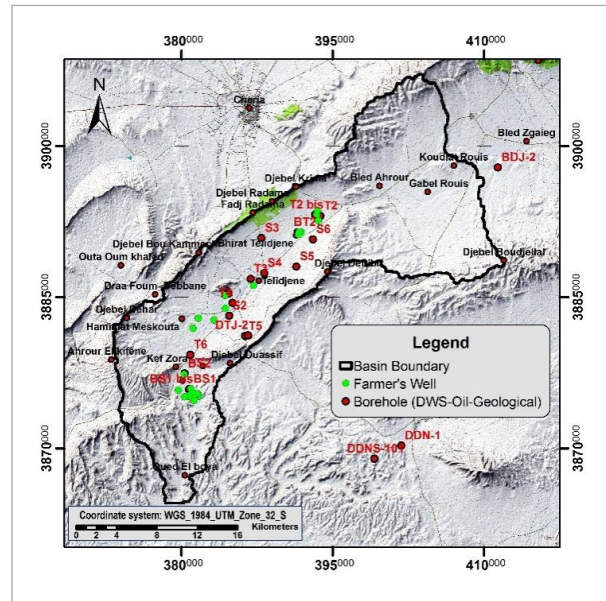
Basin are composed of intercalations of marls and limestone interrupted by the spur of Hamimat Souda built by the formation of the Aptian age. The Albian is the thickest formation; it can be seen on the surface at the level of a point abutting Hamimat Souda and on the southern slope of Hamimat Meskhouta.

Borehole and well inventory. The number of boreholes and wells inventoried in the basin is 32, the most representative of which are those intended for drinking water supply (DWS) with 4 boreholes located in the region of Bir Said (III) and next to the Telidjene city (Sector II). In addition to the mentioned boreholes, 26 wells exploited by the farmers for domestic and irrigation use that capture the alluvial groundwater were used to draw the piezometric map.

The north-eastern part of the basin (zone I), on the other hand, is supplied with potable water from the Elmalabiod basin located at the northeast limit of the perimeter. We did not find any boreholes or wells in this zone, probably due to the limited or even non-existent aquifer possibilities in this part of the basin.

Table 1 shows the distribution of the boreholes/wells by type of use and their characteristics including

Fig. 6. Boreholes and wells inventory map



exploratory drilling (geological, oil, hydraulic) and abundant wells, while Fig. 6 shows the water points inventoried in the study zone (wells/boreholes).

Table 1. Distribution of the boreholes/wells by type of use and their characteristics

Well/Bor.	Aquifer	W.D (m)	I.W.L (m)	C.W.L (m)	I.F (l/s)	C.F (l/s)	Rea. Date	E.I.S. date	Dest.	Expl. State.	Obs.
BT-1	Quat.-Cenom. Albo-Aptian	142	9.2	11.15	14.2	0	1984	2009	DWS	O.U	R.B BT2
T-2 bis	Campano-Maastrichtian	60	16.4	17.32	20	6	2005	2009	DWS	I.U	-
BS-1 bis	Maast.	100	40	40	4	4	2011	2011	DWS	I.U	-
BS2	Quat-Maast.	300	41	41.61	6	6	1987	2009	DWS	I.U	-
BT-2	Quat-Cenom.	80	24	24.3	5	5	1985	2017	DWS	I.U	-
BS-1	Maast.	150	40	40	6	6	1985	1985	DWS	O.U	R.B. BS-1 Bis
T2	Turonian	70	16.6	-	-	7.38	-	-	H.R	Aban	Flow drop
T3	Albo-Aptian	105	9.25	-	2.6	0	-	-	H.R	Aban	Flow drop
T4	Quat.-Albo.Aptian	150	Neg.	-	-	0	1982	-	H.R	-	-
T5	Santonian	-	150	-	Neg.	Neg.	1982	-	H.R	-	-
T6	Quat.-Camp. Senonian	150	17	-	-	0	1982	-	H.R	Untap	-
S2	Quat.-Cenom.	20	-	-	-	0	-	-	H.R	Untap	-
S3	Quaternary	36.7	18.4	-	-	-	-	-	H.R	Untap	-

Well/ Bor.	Aquifer	W.D (m)	I.W.L (m)	C.W.L (m)	I.F (l/s)	C.F (l/s)	Rea. Date	E.I.S. date	Dest.	Expl. State.	Obs.
S4	Quat.	45.7	31	-	-	0	1969	-	H.R	Untap	-
S5	Albo-Aptian	51	30	-	-	-	-	-	H.R	Untap	-
S6	Santonian	32	24.5	-	-	-	-	-	H.R	Untap	-
DTJ-1	Albian-Aptian	210	-	-	-	-	2013	-	G.R	-	-
DTJ-2	Santonian	300	-	-	-	-	2014	-	G.R	-	-
DDNS 101	Eocene-Maast.	350	120	-	-	2	2012	-	O.E	-	-
DDN-1	Eocene-Aptian	3175	-	-	-	-	2000	-	O.E	-	-
BDJ-2	Maast.-Upper Campanian Neocomian	3560	-	-	-	-	-	-	O.E	-	-

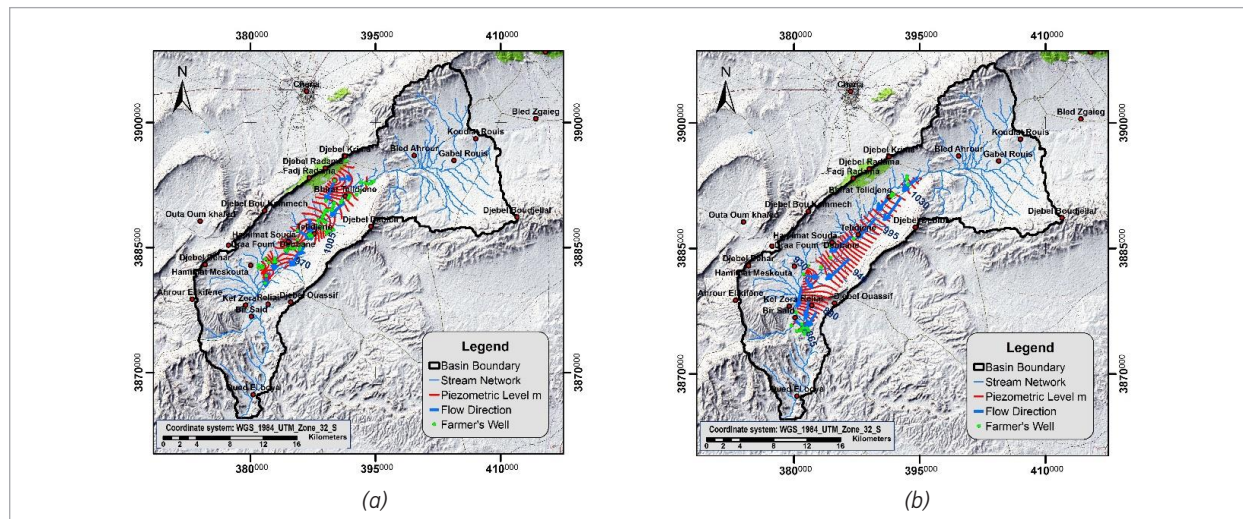
*Aband: abandoned; Bor: borehole; Camp.:Campanian. Cenom.: Cenomanian; Rea.: Realization. C.W.L: current water level, Dep: depth; Dest: destination; DWS: drinking water supply; E.I.S: enter into service; Expl: exploitation; G.R: geological research; H.R: hydrogeological research; I.F: Initial flow; I.U: in use; I.W.L: initial water level; Maast: (Maastrichtian); Neg.: negative; O.U: out of use; Ser: service; Exp.: exploitation; Obs.: observation; Neg.: negative; O.E: oil exploration; Quat.: quaternary; Untap: untapped; W.D: well depth.

Piezometry. Observation of the morphology of the piezometric map of December 1991 (Charef et al., 1991), shows that the groundwater flow generally follows a north-east to a south-east direction (Fig. 7a).

The groundwater drainage axis coincides with the course of the Wadi Telidjene, which drains surface water. Locally, two flow directions can be observed, one parallel to the axis of the wadi and the other almost perpendicular, which comes from the slopes towards the wadi, this suggests that the groundwater is

fed from the slopes. The piezometric map for November 2018 (Fig. 7b) shows that the flows are directed from north-east to south-west, a significant change in the flow direction appears at the level of Bir Said (sector III) following the change in the direction of Wadi Telidjene with also a flow direction coming from the massifs and perpendicular to the axis of the wadi. This orientation also suggests that the water table is fed by water from the peripheral massifs.

Fig. 7. Piezometric map: (a) Piezometric contour map for the watershed based on measurements from 78 wells. Modified from Charef et al. (1991); (b) Piezometric contour map for the watershed based on measurements from 26 wells (2018)



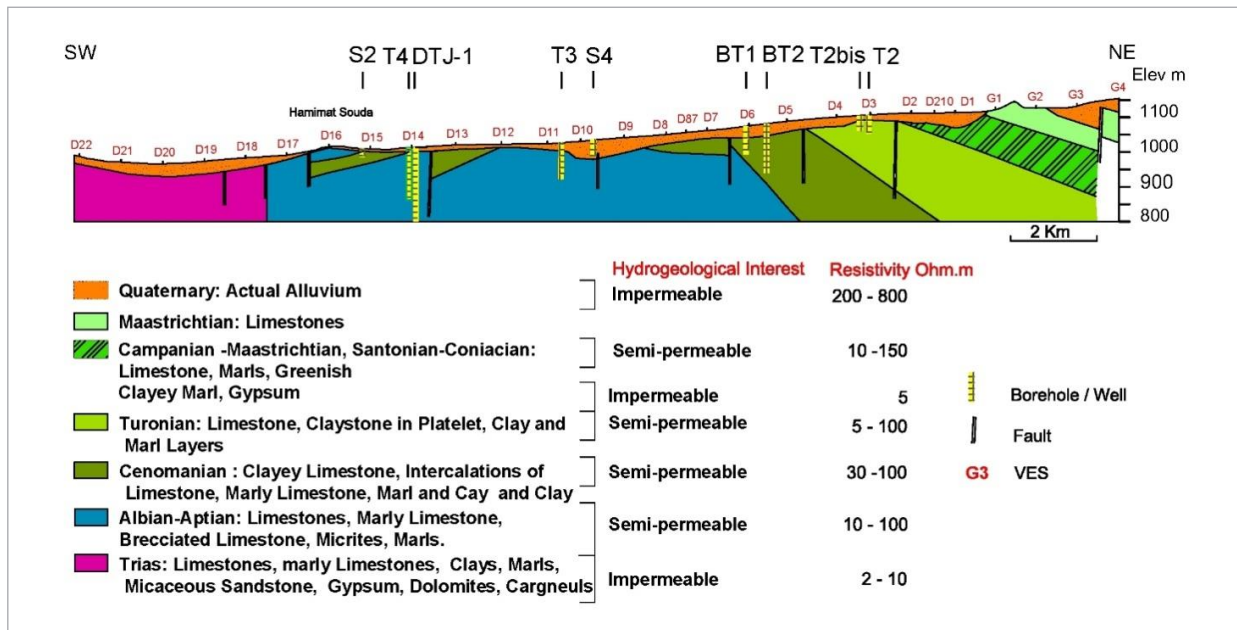
Geophysics. To determine the geometry of the existing aquifers, a geophysical survey by the Compagnie Générale de Géophysique (CGG, 1976) (Fig. 4) covering the sector (II) was used. An electrical profile of 7 vertical electrical soundings (VES) in AB 1000 was carried out in sector III of Bir Said, aiming to highlight the geometry of the superimposed aquifers of the Quaternary and Eocene-Maastrichtian, captured by the BS1 and BS2 boreholes. No investigation program has been carried out in sector I, it is due to the lack of water points to validate the results. The hydraulic and

geological borehole data shown in Table 2 were used to calibrate and reinterpret the geo-electric sections (Figs. 8 and 10) and to determine the age of the geological aquifer formations, thickness, and resistivity of the various formations.

Interpretation. Profile C' was used to trace the geological section on the axis of the anticline, as discussed in the geology section (Fig. 5).

Profiles D-G' (CGG, 1976, pl. 5, Profile D-G) (Fig. 4) allowed drawing a representative hydrogeological section in the dome part of sector II (Fig. 8).

Fig. 8. Geo-electrical cross-section along profile D-G (modified)



The geoelectric section following the D-G profiles shows the alternation, from top to bottom, of 8 geoelectric levels, of which the most important are the Mio-Plio-Quaternary, represented by recent alluvium, moderately resistant (50–150Ωm) and discordant with the Cretaceous and Triassic formations covering the dome area. The Maastrichtian limestones highlighted in the northeastern part are characterized by the highest resistivity (200–800Ωm). This horizon is of no hydrogeological interest because of the weak fracturing affecting this zone; the lowest resistivity is attributed to the Triassic formations (2–10 Ωm). Between these

two levels, there are horizons of hydrogeological interest, such as the Albo-Aptian, Cenomanian, and Turonian, with resistivities close to each other and ranging between 5 and 100 Ohm, which is due to the presence of the conductive component materialized by clays and marls in addition to carbonate formations.

Profile H' (Fig. 10) is run in Sector III. Field data were obtained from the execution of 7 vertical electrical sounding VESs that were processed by the IPI2WIN software (Fig. 9). This software allows an interactive semi-automatic interpretation that takes into account

the efficiency of the data as well as the consideration of existing geological data.

The geo-electrical section on profile H (Fig. 10) was established based on the calibrations at boreholes BS-1 and BS-2, which correspond to the following lithostratigraphy:

- ‘Quaternary’ built by recent and ancient alluvium marked by a resistivity between 10 and 150 Ωm;

- ‘Eocene’ calibrated by borehole BS1; from top to bottom it consists of limestones, marly limestones as well as an unidentified resistant layer which could be attributed to hard marly limestones. The corresponding resistivity values are 46–64 Ωm, 37–39 Ωm, and 156 Ωm;

- ‘Maastrichtian’ built up by frank limestones with a resistivity varying between 59 and 136 Ωm. The piezometric level is located at approximately 41 m; it can be detected by a drop in resistivity in the same formation.

Fig. 9. Geo-electrical cross-section along profile D–G (modified)

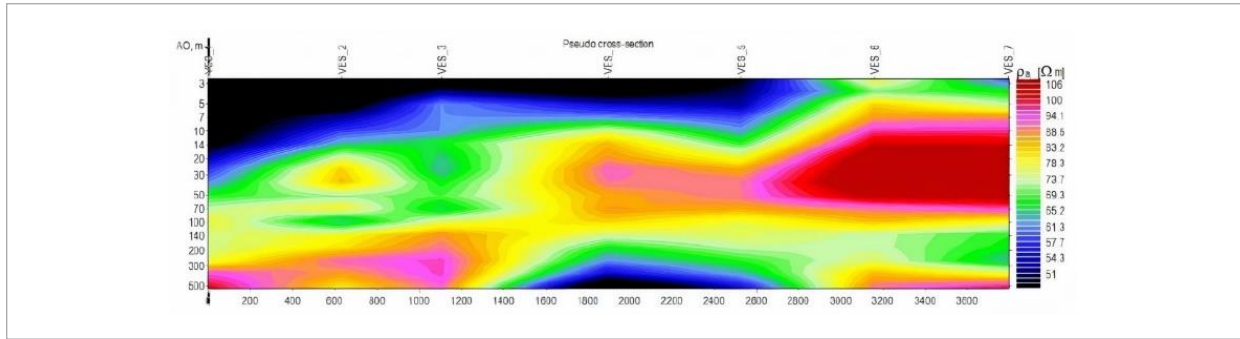
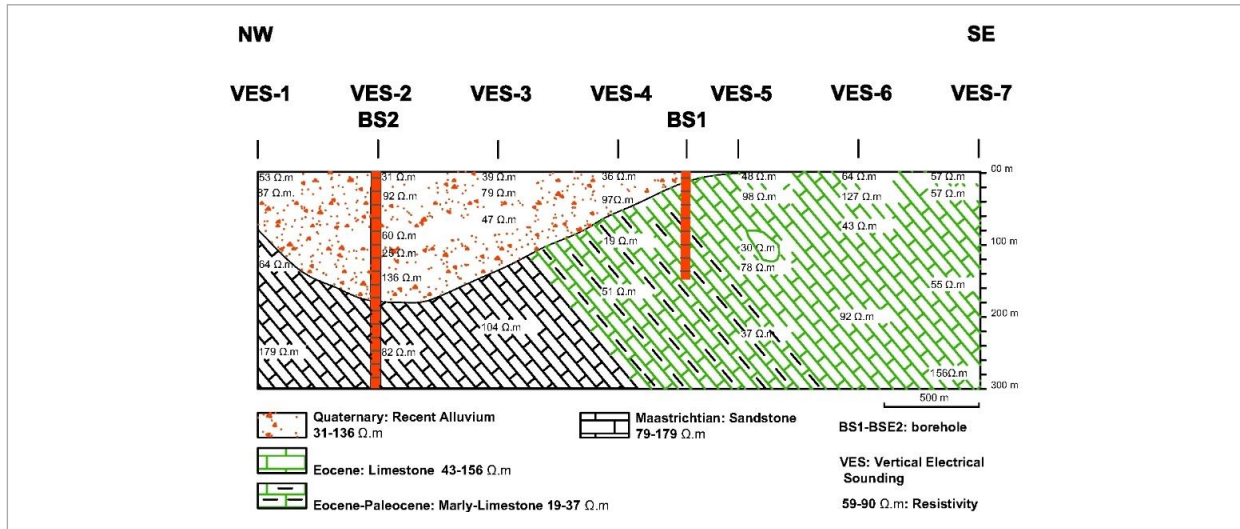


Fig. 10. Geo-electrical cross-section along profile H



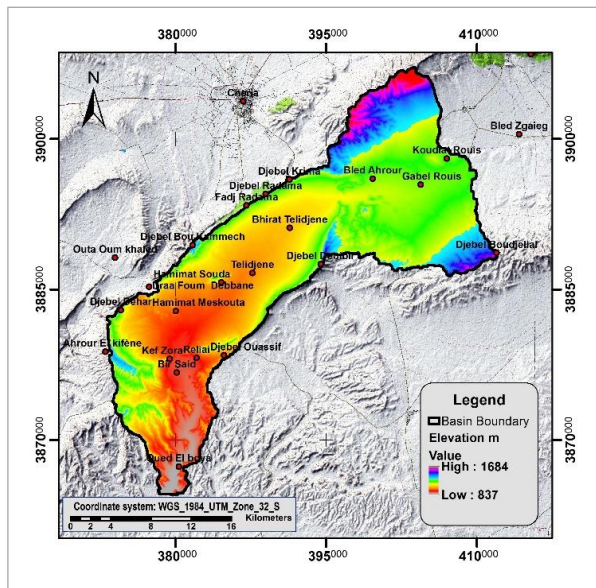
Remote Sensing Data

Remote sensing imagery and GIS analysis techniques were used to delineate the different potential recharge areas in the Telidjene Basin by identifying and

mapping the different surface factors believed to control the infiltration of surface runoff to recharge the underlying unconfined aquifers.

Processing of satellite images. For this work, the geological maps were digitized, imported into QGIS, and georeferenced. We used a multispectral Landsat 8 image. The M.N.T. digital terrain model (Fig. 11) was also used to extract the lineaments, watershed map, slope map, drainage density map, TWI map, roughness map, and curvature map.

Fig. 11. Digital elevation model of Telidjene Basin



Lineament extraction. To achieve good results, the extraction was carried out both by semi-automatic and automatic extraction of the lineaments, and their identification was performed in three steps. First, the faults were digitized using QGIS on a geological map (Fig. 12a), and automatic extraction was performed using the PCI GEOMATICA program through its Line module (Fig. 12b). Finally, the lineaments were extracted semi-automatically using the visual interpretation and the Hill-shade function of the QGIS software of the images generated from the SRTM DEM (Fig. 12c).

Artificial features, such as roads and other linear structures, were excluded from the interpreted lineaments. The extracted lineaments were superimposed on the satellite image for verification, and some of these lineaments were confirmed in the field. Finally, the QGIS and Rockworks software were used

to merge the 3 lineament maps extracted from the different methods into a single global map (Fig. 12d), and to extract the statistical parameters of the lineaments (number and lengths) to realize the rose diagram by an angular fraction of 10° .

Recharge mappings criteria and weighting. The methodology adopted was based on the use of multi-criteria analysis techniques. It consists of the delimitation of favorable groundwater recharge areas by considering the factors affecting the recharge process (Krishnamurthy, 1996; Shaban, 2020; Singh et al., 2013; Ta et al., 2011). The thematic maps were produced in two stages: the first stage was devoted to the description of the factors controlling aquifer recharge, and the second is devoted to the acquisition and classification of these factors, followed by the assignment of weights and their integration (Oularé et al., 2017).

Identification of decision criteria. The identification of the criteria determines the quality of the information generated during decision-making. Many important criteria are identified, selected, and evaluated for the establishment of different thematic maps (Jourda et al., 2006), namely slope (%), drainage density (km/km^2), lineament density (km/km^2), permeability (m/s) derived from the lithological map, land use, terrain roughness index (TRI), topographic wetness index (TWI), and curvature. It is important to point out that we did not take into account the piezometric map, which shows poor distribution of the wells inventoried in the region, nor the rainfall map because of the lack of variability of this parameter over the whole basin.

Classification, evaluation, and standardization of decision criteria. According to previous works, each decision criterion is divided into classes representing either a particular environment or an interval of values of 5 classes qualified as very weak, weak, moderate, strong, and very strong; they have been determined for this work for each criterion. To provide the most appropriate conditions for interpretation, the different classes for each criterion are standardized according to their particular influence on reservoir formation. A rating scale ranging from 1 to 10 was used (Table 2). A relationship was then established between these factors, taking into account the degree of influence of each factor on the recharge process (Shaban et al., 2006; Chowdary et al., 2009).

Fig. 12. (a) Lineament map extracted from the geological map; (b) lineament map extracted using GEOMATICA; (c) lineament map extracted using the hill-shade function of QGIS; (d) lineament full map of the Telidjene Basin

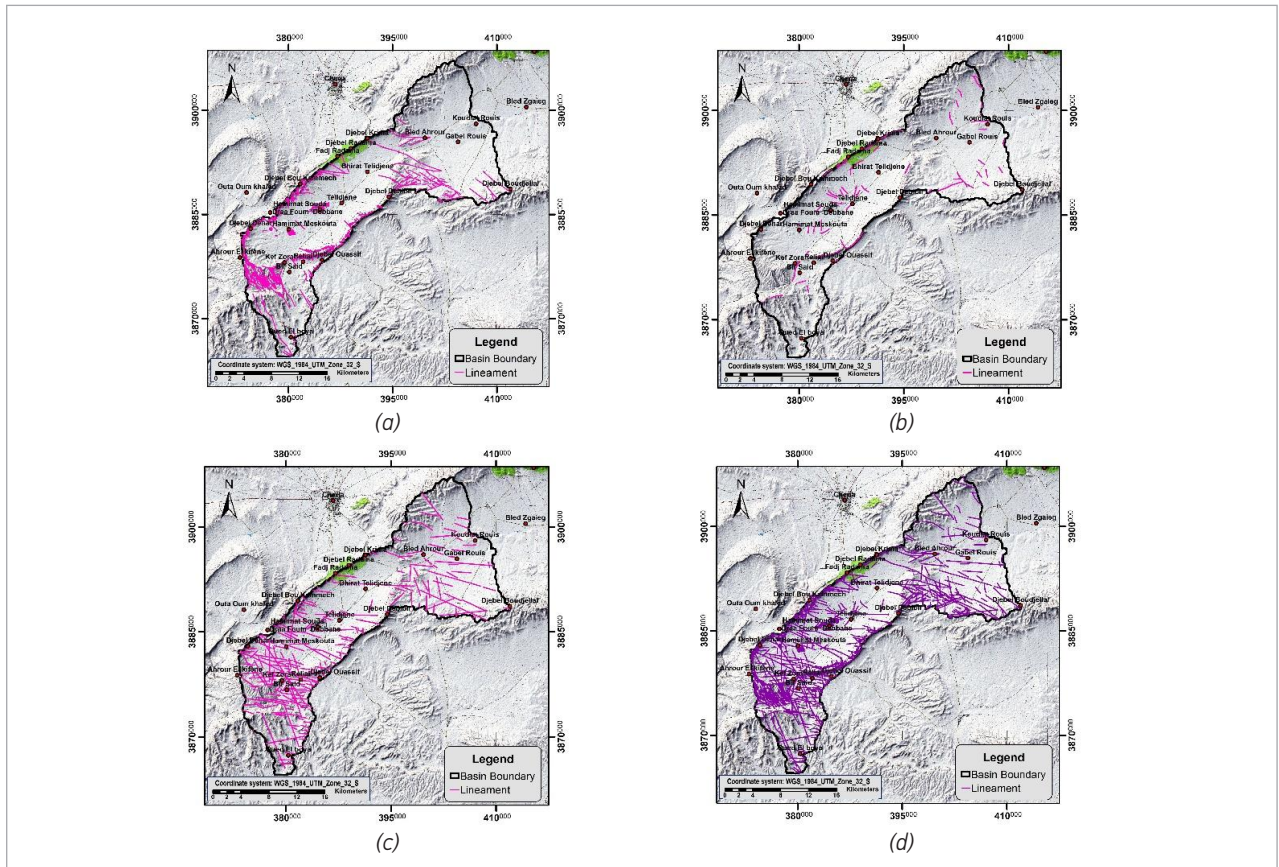


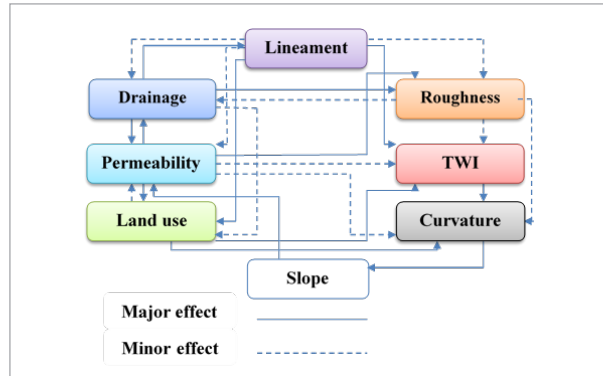
Table 2. Hydrogeological characteristics of the formations in the study area

Influence Factor	Description of Classes	Weightages	Influence Factor	Description of Classes	Weightages	Influence Factor	Description of Classes	Weightages
Lineament density	Very strong	10	Permeability	Moderate	6	TWI	Very Strong	2
	Strong	8		Weak	4		Very Weak	4
	moderate	6,5		Very Weak	2		Weak	6
	Weak	4	Land use	Very Strong	10		Moderate	8
	Very weak	2,5		Strong	6		Strong	10
Drainage density	Very strong	2,5	TRI	Moderate	8	Curvature	Very Strong	2
	Strong	6,5		Weak	4		Very Weak	4
	Moderate	8		Very Weak	2		Weak	6
	Weak	10		Very Weak	10		Moderate	8
Slope	Very strong	1	TRI	Very Weak	6		Curvature	Strong
	Strong	3		Weak	8			
	moderate	5		Moderate	4			
	Weak	10		Strong	2			

*TRI: Terrain roughness index;
TWI: Topographic wetness index

The total coefficient assigned to each factor was determined based on the relationship between the first and second factors. For a major-type relationship, a coefficient of 1 is assigned to the first factor, while a factor of 0.5 is assigned to it when the relationship is of the minor type (Fig. 13).

Fig. 13. Interactive influence of factors concerning recharge properties (modified from Shaban et al., 2006)



- (1) Lithology (permeability): 3 major and 2 minor relationships $(3 \times 1 + 2 \times 0.5) = 4$;
 - (2) Lineaments: 3 major relations $(1 \times 3) = 3$;
 - (3) Slope: 1 major relationship $(1 \times 1) = 1$;
 - (4) Drainage density: 3 major relations and 1 minor relationship $(3 \times 1 + 1 \times 0.5) = 3.5$;
 - (5) Land use: 2 major relations and 1 minor relationship $(2 \times 1 + 1 \times 0.5) = 2.5$;
 - (6) Roughness: 1 major relation and 1 minor relation $(1 \times 1 + 1 \times 0.5) = 1.5$;
 - (7) TWI: 2 minor relations $(1 \times 0.5 + 1 \times 0.5) = 1$
 - (8) Curvature: 2 minor relations $(1 \times 0.5 + 1 \times 0.5) = 1$.
- These coefficients were therefore assigned at the level of each factor according to their importance in relation to the others, applying the methodology described above. The total weights calculated for each factor are listed in Table 3.

Table 3. Assigned weightage of thematic maps according to their hydrogeological properties

	Sub-Classes of Factors	Appreciation of Classes	Weight of Sub Classes	Coefficient of Correlation	Total Weightage
Lineament Km/km ²	5.62–8.48	Very strong	10	3	30
	3.66–5.62	Strong	8		24
	2.26–3.66	moderate	6.5		19.5
	1.13–2.26	Weak	4		12
	0–1.13	Very weak	2		6
Drainage Density Km/km ²	0–0.25	Strong	2.5	3.5	8.75
	0.25–5	moderate	6.5		22.75
	5–11	Weak	8		28
	11–21	Very weak	10		35
Slope %	20–57	Very strong	1	1	1
	11–20	Strong	3		3
	05–11	moderate	5		5
	0–5	Weak	10		10
Permeability m/s	Quaternary–Sandy Miocene	Moderate	6	4	24
	Paleocene–Eocene		4		
	Upper Albian–Aptian				
	Paleocene–Eocene Maastrichtian Basal Campanian Marly Maastrichtian	Weak	4		16

	Sub-Classes of Factors	Appreciation of Classes	Weight of Sub Classes	Coefficient of Correlation	Total Weightage
	Upper Cenomanian Vraconian–Lower Cenomanian	Weak	4	4	16
	Trias	Very weak	2		8
Land Use	Wadi	Very strong	9	2.5	22.5
	Forests-Irrigated Eye – Market Gardening	Strong	8		20
	Non-irrigated crops–Pastures	Moderate	5		12.5
	Bare Soil Area with Rocky Ground	Weak	3		7.5
	Road–Built	Very weak	1		2.5
Roughness	0.11–0.36	Very weak	10	1.5	15
	0.37–0.44	Weak	6		9
	0.45–0.51	Moderate	8		12
	0.52–0.59	Strong	4		6
	0.6–0.87	Very strong	2		3
Topographic Wetness Index TWI	3.00–5.99	Very weak	2	1	2
	6.00–7.48	Weak	4		4
	7.49–9.24	Moderate	6		6
	9.25–11.6	Strong	8		8
	11.7–19.6	Very strong	10		10
Curvature	(–16.66)–(–1.07)	Very weak	2	1	2
	(–1.07)–(–0.31)	Weak	4		4
	(–0.31)–0.19	Moderate	6		6
	0.2–1.21	Strong	8		8
	1.22–15.65	Very strong	10		10

Thematic maps

Lineament density map. The presence and importance of a network of lineaments are potential indicators of water recharge (Bruel et al., 1999; Yao, 2012) since highly fractured areas have permeable locations through which water infiltrates and travels several tens of kilometers. The fracture density maps (Fig. 14a) are derived from the superimposition of 3 lineament maps produced by the QGIS and GEOMATICA programs, geological maps at scales of 1/200 000 and 1/50 000, an ASTER DEM map with a resolution of 30m, and a Landsat 8 image with a resolution of 30m. The global lineament map was processed by the QGIS program to determine fracture density; Rockworks was used to derive lineament directions.

Five classes are identified, concentrated essentially on the edges and towards the west of the watershed, very strong fracturing density, strong fracturing density, moderate fracturing density, weak fracturing density, and very weak fracturing density.

Permeability map. The permeability map was derived from existing lithological maps at scales of 1/200 000 and 1/500 000. These were digitized and then reclassified, according to the hydrogeological characteristics and nature of the natural formations of the cover (Banton and Bangoy, 1997; Castany, 1982). According to the permeability power of the rock formations (Table 4), the permeability map was reclassified into 3 main categories: moderate, weak, and very weak (Fig. 14c).

Table 4. Permeability of the geological formations of the Telidjene Basin (modified from Banton and Bangoy, 1997)

Age	Lithology	Permeability m/s	Permeability Class
Quaternary	Limestone screes, alluvial deposits, silts, alluvial fans	-11 to -5	Moderate
Vraconian–Lower Cenomanian	Marly limestone, marl, marl, and gypsum	-11 to -9	Weak
Upper Cenomanian	Marl, sandy marl, gypsum	-11 to -9	Weak
Campanian basal marly Maastrichtian	Gypsum, marls	-11 to -9	Weak
Sandy–Miocene	Siliceous conglomerates, sandy clays with carbonate particles	-11 to -4	Moderate
Paleocene–Eocene	Phosphatic limestone and flint	-11 to -4	Weak
Maastrichtian	Limestone	-3 to 0	Weak
Upper Albian–Aptian	Limestones, marly limestones, brecciated limestone, micrites, marls	-11 to -4	Moderate
Trias	Motley clays, marls, micaceous sandstone, gypsum, dolomites, cargneuls	-12 to -6	Very weak

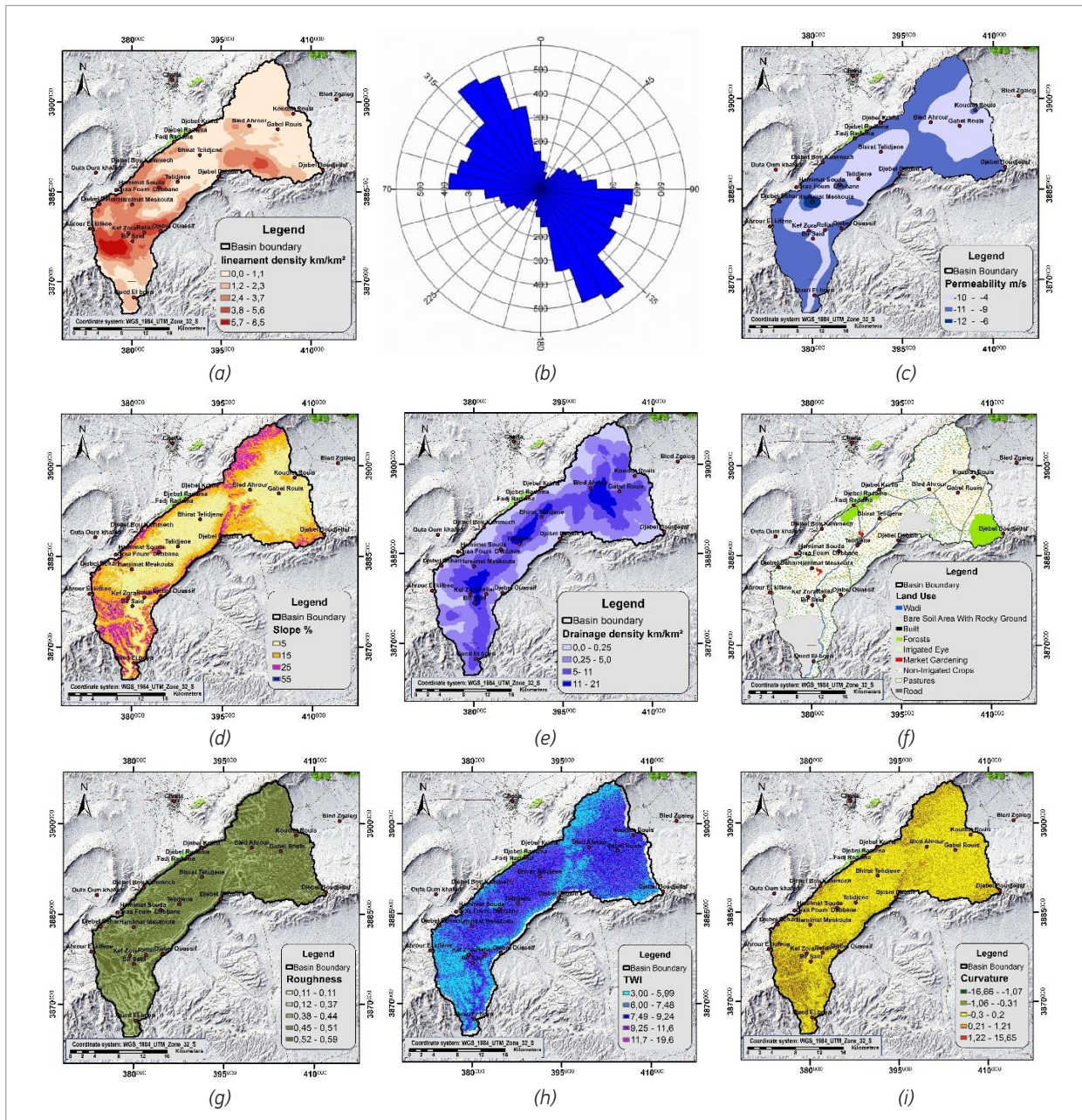
This parameter allowed us to identify 5 classes concentrated essentially on the edges and towards the west of the watershed, very strong fracturing density, strong fracturing density, moderate fracturing density, weak fracturing density, and very weak fracturing density.

Slope. The slope map was created using a digital elevation model (DEM). The examination of the slope values led to the identification of 4 classes: steep, medium, shallow, and very shallow slopes (Fig. 14d). On the mountains, the slope is very steep, which favors high surface runoff and less water infiltration, which results in a lower groundwater recharge capacity (MachiwaL et al., 2011), and in the foothills, we found a medium to the low slope. The lowest values were recorded in the areas between the mountain foothills and plains, which are the areas that favor infiltration into the soil (reduce runoff) and have a higher groundwater recharge capacity due to high rainwater retention. The lowest values were recorded in the areas between the mountain foothills and plains, which promote infiltration into the soil (reduce runoff) and have a higher groundwater recharge capacity due to high rainwater retention.

Drainage density map. In the study of the erosion processes established by Horton 1945, drainage density is lower as the infiltration capacity is risen and varies in the same direction as the stream and the opposite direction of the underground flow. According to Greenbaum (1985), the transmissibility of the terrain appears to be the dominant factor in drainage density, which is one of the most important indicators of hydrogeological characteristics. The drainage network for the study area was created from the SRTM global elevation data, and the drainage density values were grouped into four drainage density classes (Fig. 14e): very low, low, medium, and high

Land use map. The land-use map (Fig. 14f) was obtained by digitizing the land use map of Tébessa edited by the National Institute of Soil, Irrigation, and Drainage (INSID, 2011). The original map has 8 classes: forests, roads, wadi, built, dry crops, non-irrigated crops, market gardening, irrigated eye cultivation, bare soil area with rocky ground, and pastures. Several studies have shown that changes in land use strongly influence groundwater recharge (Roose, 1973; Owuor et al., 2016). According to the influence of the nature of the occupant on the recharge, the land-use map

Fig. 14. Thematic maps: (a) Lineament density; (b) rose diagram of the major lineament orientations; (c) permeability; (d) slope; (e) drainage density; (f) land use; (g) terrain roughness index; (h) topographic wetness index; (i) curvature.



has been reclassified into 5 zones ranging from very strong to very weak.

Terrain roughness index TRI. The calculation of the roughness index allows us to characterize the different

types of relief. Roughness characterizes the aspect of the surface, which can be smooth or modeled in multi-form micro-relief. It acts as a surface holding agent on gentle slopes; it favors water storage and slows

down runoff (Magunda, 1997; Onstad et al., 1984; Kamphorst, 2000). Fig. 14g shows the terrain roughness map of the Telidjene Basin with values ranging from 0.11 to 0.87. The values were reclassified into 5 categories: high weights assigned to low roughness values, and vice versa.

Topographic wetness index TWI map. This index combines the local upstream contribution area and the slope. It is generally used to measure the effect of topography on hydrological processes (Beven and Kirkby, 1979; Nair et al., 2017) (Fig. 14h). It is commonly used to measure and evaluate the spatial distribution of moisture conditions and requires only the elevation data to be well distributed over the study area. The calculated model is independent of time and is a static representation of the landscape.

Curvature map. Curvature is the quantitative expression of the nature of the surface profile and can be concave or convex. Water tends to decelerate and accumulate in convex and concave profiles (Reiffsteck, 2003). The curvature ranges in the study area vary from 4.33 to -2.46. The values are reclassified into 5 classes such as -2.46 to -1.10, -1.10 to 0.25, 0.25 to 1.61, 1.61 to 2.97 and 2.97 to 4.33. High weight is assigned for a high curvature value and vice versa. Fig. 14i shows the curvature map of the Telidjene Basin.

Results and Discussion

Results

Lineaments. Analysis results are presented in the form of a lineament map, a lineament density, and a rose diagram. The lineament map shows a heterogeneous lineament distribution (Fig. 4).

As shown in (Fig. 14b), the main predominant directional families are "NW-SE" and "E-W", respectively. The "NW-SE" family is marked throughout the region and is subparallel to the major Tébessa-Morsott ditch accidents, followed by the "E-W" direction, which is predominant mainly in the south-western part of the watershed. The latter comes from two other sets of lineaments, although to a lesser degree than the first two directions, with a "NE-SW" orientation and "NNW-SSE" to N-S orientation.

Aquifers. The identification of the aquifer systems was elaborated based on the lithological data of the outcropping geological formations, and the results of the existing drilling works, allowing the definition of the main aquifer systems. The geophysical study carried out by the Compagnie Générale de Géophysique was used to highlight the extent of the alluvial aquifer of the part of the eroded dome with a diapiric core (the Telidjene Anticline). The aquifer systems we defined in the Telidjene watershed are shown in Fig. 8 and Fig. 10 and are numbered as follows:

- (1) The aquifer of the Plio-Quaternary. Consisting mainly of alluvium, gravel, and pebbles, it is generally located along the Wadi of Telidjene, the plains, and the dejection cones, it is most exploited by farmers. This aquifer, located in the dome area, was studied in detail by CCG (1976). The bedrock of this layer is composed of marls, hard limestones, and sometimes clays, which is due to the lateral heterogeneity of the geological structure with varied nature.
- (2) The two-layer aquifer of the Bir Said region III. It is the result of the superposition of Quaternary formations built by ancient and recent alluvial deposits and Maastrichtian limestones, with more or less dense fissured and karstic networks. The Maastrichtian aquifer is confined; it has a hard roof without cracking, with a thickness varying from 20 to 40m. According to the boreholes DDNS-101, DDN-1, and BDJ-2; the thickness of the Maastrichtian limestones is approximately 200m; water inflows are observed between 41 and 85 m deep, which shows that the water of these aquifers circulates under pressure.
- (3) Turonian aquifer. This zone presents a confined karstic aquifer in fissured and karstified limestones made up of hard limestones intercepted by borehole T2.
- (4) Cenomanian Aquifer. This aquifer is exploited by drilling BT2, it is a confined aquifer approximately 30 m thick in fissured marly limestones, with a roof built by marly formations.
- (5) Albo-Aptian Aquifer. The diversity of hydrogeological conditions, essentially related to the geological structure and properties of the Albo-Aptian rocks,

shows a change in the water resources in this area. T3 intersecting this zone shows saturated horizons in limestones, and marly limestones form a confined aquifer system. However, information on the deposit of this aquifer and its hydraulic link is insufficient and often confused to allow an estimation of the exploitation of the zone. At a distance of 3,000 m towards the southwest, drill T4 intercepting the marly and marly limestone formations has proven to be unproductive for pumping, which indicates that these limestone intercalations are impermeable and sterile. It should be recalled that borehole T3 has been stopped for several years due to a drop in the flow rate, and at the time of drilling, the flow rate of this borehole was 2.6 L/s.

Comparison of piezometric maps for the period 1991–2018. In general, the current flow direction was unchanged compared with that in 1991. The orientation is still from the north-east to the south-west, the extension of the isopiezies of November 2018 on sector III of Bir Said confirms that the direction of the flow follows that of the main wadi.

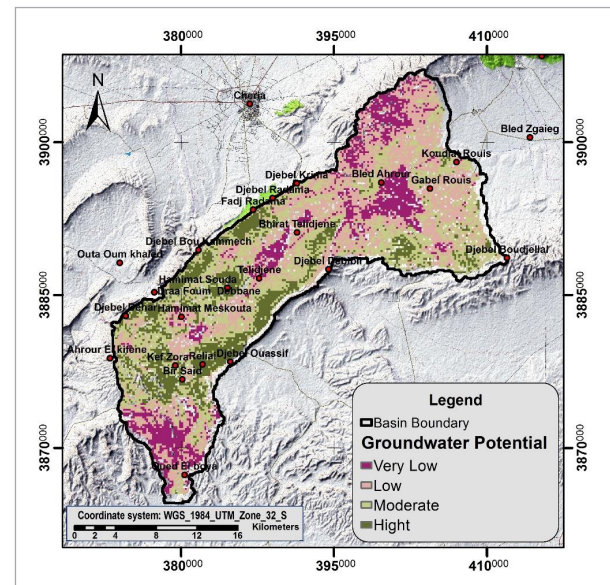
A decrease in the piezometric level was observed between 1991 and 2018 on the entire plain. Hamimat Meskhouta and Hamimat Souda are the sectors where the greatest drop in the piezometric level can be observed at 59.5 and 58 m, respectively. In the remaining sectors, the average variation value between 1991 and 2018 varies between 30 and 44 m. Generally speaking, the piezometric level has decreased significantly, which has led to the cessation of most of the wells inventoried in the 1991 period (Charef et al., 1991).

Groundwater potential recharge zones map. The weighted overlay of the different thematic maps made it possible to construct a synthesis map showing the locations of areas potentially favorable to groundwater recharge (Fig. 15).

This map, which was classified into 4 categories, shows the following:

The high potential class represents 16% of the basin surface; it is dominated by very strong fracturing and carbonate formations, which are mainly located in inaccessible areas and are impacted by very strong fracturing.

Fig. 15. Groundwater potential recharge zones map



The class with moderate potential represents 32% of the total surface area of the basin and meets well to moderate drainage conditions.

The low and the very low potential classes represent 32% and 20% of the occupied proportion, respectively. These zones are located in areas with high and moderate drainage density, in the north-eastern part, as well as in the south-western parts of the landforms, which are underlain by weakly fractured limestone.

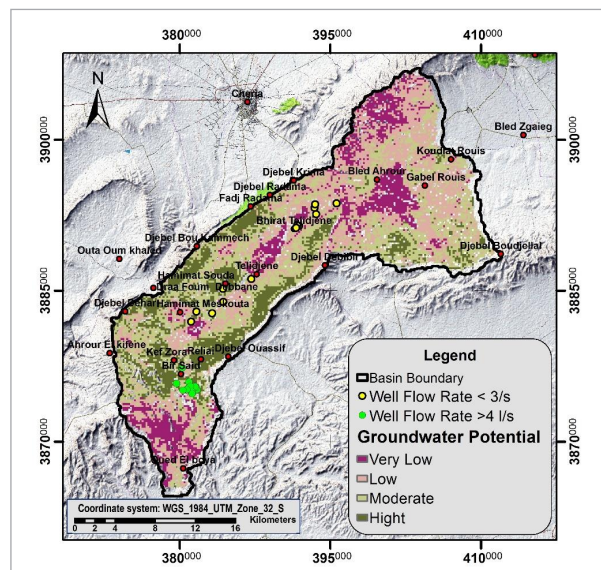
According to these statistics, the most favorable zone is mainly located in inaccessible areas and is impacted by very strong fracturing. The area with moderate potential occupied 32% of the land. It can be concluded that the region of Telidjene offers strong to moderate potentialities in groundwater and that this zone covers approximately 48% of the territory.

Validation of the results of the groundwater potential recharge zones map. Based on the results of the hydrogeophysical study, we were able to obtain information on the distribution and structure of the Quaternary water table as well as the carbonate formations (Maastrichtian and Eocene). This information allows measuring the coherence of the remote sensing results and the hydrogeophysical study, as the water table presents unconfined horizons controlled by recharge.

The hydrogeophysical study showed that the Bir Said (sector III) is the most promising area for the presence of groundwater. This area is characterized by a high groundwater potential, confirmed by the presence of a large saturated thickness of the Quaternary aquifer. According to the synthesis map, this area is marked by a strong to moderate potential, as well as the most productive wells and boreholes, which confirms that the area benefits from a recharge coming from the alluvial formations as well from the edges materialized by fractured limestone.

Therefore, to validate the map of potential recharge areas, it was overlaid on the 26 existing boreholes and wells in the basin. It was found that wells with a flow rate of 3 l/s or less were superimposed on the low to very low class. The water points with a flow rate greater than 4 l/s are superimposed on the moderate to high classes, suggesting that this increase in flow rate, particularly in this part, is due to direct infiltration of the alluvial cover and a supply from the carbonate edges, revealing a high potentiality according to the summary map (Fig. 16).

Fig. 16. Groundwater potential recharge zones superimposed to the water points



Discussion

Lineament. The presence of lineaments could indicate the location of brittle deformation that could also be

responsible for improved permeability and enhanced groundwater localization (Mpofu et al., 2020); the study confirmed a strong relationship between faulting and potential recharge areas. In general, the majority of the productive wells were located in a corridor marked by a high density of fractures (Figs. 12d and 14a) that extends from the Draa Foug Debbane passing through Kef Zora, Reliai, up to the outlet of the Basin. This fracturing constitutes a zone of weakness where erosion is more active and constitutes a privileged place for the development of ravines constituting the axes of gathering and channeling rainwater. It is the only zone (sector III) where the dip direction of the Eocene and Maastrichtian calcareous layers follows the water table flow direction and is favorable for feeding the alluvial water table. This process helps explain the stability of the piezometric level in Sector III. It should be noted that the BS1 borehole drilled in 1995 intercepts the alluvial formations and Maastrichtian limestone (Table 1). Its current piezometric level is 41.60 m with an insignificant drawdown of 0.60m compared with the initial level; this information confirms the result of the groundwater potential recharge map. In fact, there is a good response of the recharge to precipitation by direct infiltration from the alluvial cover and the fractured limestone outcrops in this sector.

Aquifers. Influenced by the network of lineaments and fractures, the aquifer system in the Telidjene Basin is compartmentalized into two structures: an anticlinal structure occupying the dome region and a synclinal that is positioned south-west of the basin. These structures control the groundwater flow (Chelih et al., 2018) by the presence of lateral discontinuities due to the change of the geological facies as well as the series of faults of "NW-SE" and "E-W" directions which appear perpendicularly to the direction of the flow in the dome region. The same fault family acts as a drain and promotes infiltration when parallel to the flow direction.

Although this study presents an effective means of initiating the aquifer geometry of the Telidjene Basin, it is insufficient to lead to a hydrodynamic characterization of the aquifer infrastructure. Future research will need to deepen the knowledge around this issue.

Groundwater potential recharge zones. Based on the methodology presented, the study area was classified

into 4 potential recharge zones, namely strong, moderate, weak, and very weak, covering 16%, 32%, 32%, and 20% of the study area, respectively. Although a large part of the study area (48%) has a high to moderate recharge capacity, it can be seen that groundwater resources are somewhat limited in the study area, since that the most favorable class is located in inaccessible limestone outcrops where extension and dip are not favorable for flow towards the water table but rather towards the adjacent basins.

The high potential class also occupies the areas of slope breaks, from which we observe the abundance of alluvial fans that present privileged places for infiltration due to their coarse granulometry (Amelot et al., 2003).

It should be remembered that the 1991 piezometric map showed a flow direction perpendicular to the axis of the main talweg, which confirms that recharge occurs through direct infiltration of the alluvial fans and not from the limestone outcrops where dip and extension of the layers are opposite to the direction of flow of the water table. The presence of marl-clay intercalations in the edge formations in contact with the water table aquifer also makes its feed difficult.

In the present study, the 8 parameters that were retained are the most important in determining the recharge zones based on the experience of previous work. However, topographic wetness index and curvature maps show similar zoning; as per Table 3, the weight assigned to each factor according to its hydrogeological characteristics is the same, which means that these indicators are equal. Overestimation of factor weights could also be done if there is a dependency relationship between the parameters. These observations lead to the suggestion of statistical correlation analysis to measure the degree of dependency of the factors, avoiding redundancy and finding the most discriminatory factors for predicting the recharge phenomenon by the multi-criteria method (Pinson and Stollsteiner, 2016).

Piezometry. The piezometric levels of the boreholes capturing the aquifer horizons under the Quaternary cover in the dome and Bir Said regions show stability over time (Table 1). However, it was not possible to establish a mapping for these deep horizons due

to the insufficient number of monitoring wells. This missing information did not provide better knowledge of the interactions of these deep horizons with surface waters nor did it provide information on understanding their behavior and capabilities.

Conclusions

The present study demonstrates the effectiveness of integrating remote sensing with hydrogeophysics to identify the most favorable areas for groundwater exploitation in the Telidjene region. The study showed that the alluvial aquifer extends over the entire basin plain and benefits from a weak to moderate recharge in the dome region where an anticlinal structure with complex geology is encountered; in the south-west, it benefits from a recharge by the edges of the calcareous formations of Maastrichtian and Eocene age and deposits in normal contact, thus forming a two-layer aquifer.

The exploitation of geoelectrical data also shows that this water table is deposited in an unconformity on aquifer horizons of Cretaceous age in the dome region. These are the Turonian, Cenomanian, and Albo-Aptian aquifers, where resources can change within the same aquifer due to the existence of a marly component alternating with the limestones, as well as the complexity of their geological properties and structure. These aquifers require detailed geophysical and hydrogeological investigations to determine their geometry, especially their lateral extension, recharge conditions, and hydrodynamic characteristics.

A multidisciplinary methodology was also used to delineate potential groundwater recharge areas, which is a GIS-based multi-criteria decision-making technique. The proposed technique, which is widely used, uses several parameters depending on the hydrogeological context. These parameters made it possible to evaluate the potential for groundwater recharge. The study used satellite data (SRTM data), geological, and land use mapping to prepare 8 thematic maps, namely, slope, drainage density, permeability, fracturing, land use, roughness, topographic wetness index, and curvature.

The map of potential recharge areas was made based on the mapping of the 8 thematic layers that were reclassified to achieve the best result. A weight is assigned to them according to the influence of each factor on the recharge capacity of the land and its relative importance to groundwater. Weights were assigned to the thematic layers according to their influence on recharge as well as the relationship

In summary, the results of this study demonstrated the efficacy of combining remote sensing techniques and hydrogeophysics to produce a reliable decision tool on groundwater potential based on geoelectrical parameters, accessible morphometric measurements, and induced by subsurface datasets. The study made it possible, for the first time, to shed light on the hydrogeological context of the Telidjene Basin and to improve knowledge about the aquifer system as well as its recharge conditions. Remote sensing work made it possible to update the geological map of the region by

creating a new lineament map, while the processing of hydrogeophysical data facilitated the establishment of new geological and hydrogeological sections. The maps obtained through this technique can be used by local authorities and managers to select suitable sites for drilling new wells, and it can also help in formulating effective groundwater development strategies for the study area to ensure the long-term sustainability of this vital resource.

The obtained results deserve to be refined by other studies, in particular by integrating the “geophysical” parameter in the multi-criteria analysis and treating it in a GIS environment to allocate potential groundwater areas by moving from a qualitative approach to a quantitative approach. Knowledge of the geometry of the deep aquifers in the dome area needs to be improved to better control the exploitation of the locations.

{Gorauskiene, 2006, Eco-design methodology for electrical and electronic equipment industry}

References

- Amelot, F., Delannoy, J. J., and Nicoud, G. (2003). L'édification des cônes de déjection en zone de montagne: intérêts paléoenvironnemental et hydrogéologique, contribution typologique (Building of alluvial fans in mountain regions palaeoenvironmental and hydrogeological interest, contribution to a typology). *Quaternaire*. 14/4, 253-263. <https://doi.org/10.3406/quate.2003.1746>
- Arulbalaji, P., Padmalal, D., and Sreelash, K. (2019). GIS and AHP techniques based delineation of groundwater potential zones: a case study from southern western Ghats, India. *Scientific Reports*, 9(1), 1-17. <https://doi.org/10.1038/s41598-019-38567-x>
- Baali, F. (2007). Contribution à l'étude hydrogéologique, hydrochimique et Vulnérabilité d'un système aquifère karstique en zone semi aride. Cas du plateau de Chéria NE Algérien (Contribution to the hydrogeological, hydrochemical and vulnerability study of a karstic aquifer system in a semi-arid zone. Case of the NE Algerian Chéria plateau) (Doctoral dissertation, Université de Annaba-Badji Mokhtar).
- Banton, O. and Bangoy, L. M., (1997). Hydrogéologie : Multi-science Environnementale des Eaux Souterraines. Persse de l'Université du Québec/AUPELF, (460p).
- Beven, K. J., and Kirkby, M. J. (1979). A physically based, variable contributing area model of basin hydrology/Un modèle à base physique de zone d'appel variable de l'hydrologie du bassin versant. *Hydrogeological Sciences Journal*, 24/1, 43-69. <https://doi.org/10.1080/02626667909491834>
- Breusse, J. (1963). La prospection géophysique des eaux souterraines (Geophysical prospecting for groundwater). *La Houille Blanche*, 4, 407-413. <https://doi.org/10.1051/lhb/1963027>
- Bruel, T., Petit, J. P., Massonnat, G., Guerin, R., and Nolf, J. L. (1999). Relation entre écoulements et fractures ouvertes dans un système aquifère compartimenté par des failles et mise en évidence d'une double porosité de fractures (Relationship between flows and open fractures in a faulted aquifer system and evidence of double fracture porosity). *Bulletin de la Société Géologique de France*, 170(3), 401-412.
- Castany, G. (1982). Principes et Méthodes de l'Hydrogéologie (Principles and Methods of Hydrogeology). Université de Pierre et Marie Curie (Paris VI), Collection Dunod, Université-Bordas, 233p.
- Charef, N., Bocharia, H., Tounsi, B., (1991). Etude hydrogéologique préliminaire dans le bassin d'Ain Telidjene (Preliminary hydrogeological study in the Ain Telidjene basin). *Mémoire de D.E.U.A, Université Larbi Tebessi, Tébessa, Algérie*, 57p.
- Chelih, F., Fehdi, C., and Khan, S. (2018). Characterization of the Hammamet basin aquifer (north-east of Algeria) through geochemical and geostructural methods and analysis. *Journal of*

- Water and Land Development. <https://doi.org/10.2478/jwld-2018-0023>
- CGG (1976). Etude géophysique dans la région de Tébessa, Région des dômes, Bassin de Telidjene (Geophysical study in the region of Tébessa, Domes region, Telidjene basin), 1976
- Chowdary, V. M., Ramakrishnan, D., Srivastava, Y. K., Chandran, V., and Jeyaram, A. (2009). Integrated water resource development plan for sustainable management of Mayurakshi watershed, India using remote sensing and GIS. *Water Resources Management*, 23/8, 1581-1602. <https://doi.org/10.1007/s11269-008-9342-9>
- Dubourdieu, G., Durozoy. (1950). Observation tectonique dans les environs de Tébessa et de l'Ouenza (Algérie) (Tectonic observation in the surroundings of Tébessa and Ouenza. Algeria). *Bulletin de la société géologique de France* 5, 257-266. <https://doi.org/10.2113/gssgfbull.S5-XX.4-6.257>
- ENERGOPROJECT-ENHYD (2002). Etude de la petite et moyenne hydraulique agricole de l'Algérie du nord (Study of the small and medium agricultural hydraulics of northern Algeria), Mission 1- Dossier 2- Secteur 4
- Gonçalves, J. A. C., Pereira, P. H. R., and Vieira, E. M. (2020). Evaluation of the groundwater recharge potential using GIS multi-criteria data analysis: a case study from district of Itabira, Minas Gerais, southeastern Brazil. *Ciência e Natura*, 42, 84. <https://doi.org/10.5902/2179460X40433>
- Gouaidia, L. (2008). Influence de la lithologie et des conditions climatiques sur la variation des paramètres physico-chimiques des eaux d'une nappe en zone semi aride, cas de la nappe de meskiana nord est algerien (Influence of lithology and climatic conditions on the variation of physico-chemical parameters of groundwater in a semi-arid zone, the case of the Meskiana aquifer in north-eastern Algeria) (Doctoral dissertation, Annaba).
- Greenbaum, D. (1985). Review of remote sensing applications to groundwater exploration in basement and regolith. *British geological survey*, wc/og/85/i.
- Gyeltshen, S., Tran, T. V., Teja Gunda, G. K., Kannaujiya, S., Chatterjee, R. S., and Champatiray, P. K. (2020). Groundwater potential zones using a combination of geospatial technology and geophysical approach: case study in Dehradun, India. *Hydrological Sciences Journal*, 65(2), 169-182. <https://doi.org/10.1080/02626667.2019.1688334>
- Haouchine, A., Abderrahmane, B., Haouchine, F. Z., and Nedjai, R. (2010). Cartographie de la recharge potentielle des aquifères en zone aride (Mapping the potential recharge of aquifers in arid zones). *Eurojournals*, 45/4, 1-13.
- Horton, R. E. (1945) Erosional development of streams and their drainage basins: hydrophysical approach to quantitative morphology. *Bulletin of Geological Society of America*, 56(3), 275-370. [https://doi.org/10.1130/0016-7606\(1945\)56\[275:E-DOSAT\]2.0.CO;2](https://doi.org/10.1130/0016-7606(1945)56[275:E-DOSAT]2.0.CO;2)
- INSID (2011). Carte de l'occupation du sol de l'Algérie Au 1/50 000 pour le nord et au 1/200 000 pour le sud.2011 (Land use map of Algeria At 1/50 000 for the north and at 1/200 000 for the south .2011).
- Jourda, J.P., Saley, M.B., Djagoua, E.V., Kouame, K.J., Biemi, J. and Razack, M. (2006). Utilisation des données ETM+ de Landsat et d'un SIG pour l'évaluation du potentiel en eau souterraine dans le milieu fissuré précambrien de la région de Korhogo (nord de la Côte-d'Ivoire) (Use of Landsat ETM+ data and GIS for groundwater potential assessment in the Precambrian fractured environment of the Korhogo region (northern Côte d'Ivoire)): approche par analyse multicritère et test de validation. *Revue de Teledetection* 5, 339-357.
- Kamphorst, E. C., and Jetten, V., Guerif, J., Pitk A` NEN, J., Iversen, B. V., Douglas, J. T., and Paz, A. (2000). Predicting depressional storage from soil surface roughness. *Soil Science Society of America Journal*, 64(5), 1749-1758. <https://doi.org/10.2136/sssaj2000.6451749x>
- Krishnamurthy, J., venkatesa kumar, N., Jayaraman, V., and Manivel, M. (1996). An approach to demarcate ground water potential zones through remote sensing and a geographical information system. *International Journal of Remote Sensing*, 17(10), 1867-1884. <https://doi.org/10.1080/01431169608948744>
- Machiwal, D., Jha, M.K., and Mal, B.C. (2011). Assessment of groundwater potential in a semi-arid region of India using remote sensing, GIS and MCDM techniques. *Water Resour.Manag.* 25, 1359-1386. <https://doi.org/10.1007/s11269-010-9749-y>
- Magunda, M. K., Larson, W. E., Linden, D. R., and Nater, E. A., (1997). Changes in microrelief and their effects on infiltration and erosion during simulated rainfall. *Soil technology*, 10(1), 57-67. [https://doi.org/10.1016/0933-3630\(95\)00039-9](https://doi.org/10.1016/0933-3630(95)00039-9)
- Mogaji, K. A., and Omobude, O. B. (2017). Modeling of geoelectric parameters for assessing groundwater potentiality in a multifaceted geologic terrain, Ipinsa south-west, Nigeria-A GIS-based GODT approach. *NRIAG Journal of Astronomy and Geophysics*, 6(2), 434-451. <https://doi.org/10.1016/j.nrjag.2017.07.001>
- Mohamaden, M. I. I., El-Sayed, H. M., and Mansour, S. A. (2017). Combined application of electrical resistivity and GIS for groundwater exploration and subsurface mapping at north-east Qattara Depression, western Desert, Egypt. *Egyptian Journal of Basic and Applied Sciences*, 4(1), 80-88. <https://doi.org/10.1016/j.ejbas.2016.10.003>
- Moreira, C. A., Rosolen, V., Furlan, L. M., Bovi, R. C., and Masquelin, H. (2021). Hydraulic conductivity and geophysics (ERT) to as-

- sess the aquifer recharge capacity of an inland wetland in the Brazilian Savanna: Hydraulic conductivity and geophysics (ERT) to assess the aquifer recharge capacity of an inland wetland in the Brazilian Savanna. *Environmental Challenges*, 5, 100274. <https://doi.org/10.1016/j.envc.2021.100274>
- Mpofu, M., Madi, K., and Gwavava, O. (2020). Remote sensing, geological, and geophysical investigation in the area of Ndlambe Municipality, Eastern Cape Province, South Africa: Implications for groundwater potential. *Groundwater for Sustainable Development*, 11, 100431. <https://doi.org/10.1016/j.gsd.2020.100431>
- Nair, H. C., Padmalal, D., Joseph, A. and Vinod, P. G., (2017). Delineation of Groundwater Potential Zones in River Basins Using Geospatial Tools: An Example from Southern western Ghats, Kerala, India. *Journal of Geovisualization and Spatial Analysis* 1, 5. <https://doi.org/10.1007/s41651-017-0003-5>
- Nicaise, Y., Bertrand, A. H., Marc, Y. T., and George, A.,(2019) Apport De La Télédétection Et De La Géophysique Dans La Cartographie Des Fractures Hydrauliquement Actives En Zone De Socle Au Centre-Ouest Du Benin(Contribution of Remote Sensing and Geophysics to the Mapping of Hydraulically Active Fractures in the Central-Western Region of Benin). <https://doi.org/10.19044/esj.2019.v15n27p426>
- Ogungbade, O., Ariyo, S. O., Alimi, S. A., Alepa, V. C., Aromoye, S. A., and Akinlabi, O. J. (2021). A Combined GIS, Remote Sensing And Geophysical Methods For Groundwater Potential Assessment Of Ilora, Oyo Central, Nigeria. <https://doi.org/10.21203/rs.3.rs-267236/v1>
- Onstad, C. A., Wolfe, M. L., Larson, C. L., and Slack, D. C. (1984). Tilled soil subsidence during repeated wetting. *Transaction of the ASAE*, 27(3), 733-0736. <https://doi.org/10.13031/2013.32862>
- Oularé, S., Adon, G., Akpa, L., Mahamn bachir S., Kouamé F., Therrien R., (2017). Identification Des Zones Potentielles De Recharge Des Aquifères Fracturés Du Bassin versant Du N'zo (Ouest De La Côte d'Ivoire) : Contribution Du SIG Et De La Télédétection (Identification of Potential Recharge Areas of Fractured Aquifers in the N'zo Watershed (western Côte d'Ivoire): Contribution of GIS and Remote Sensing). *European Scientific Journal*. 13, 192-217. <https://doi.org/10.19044/esj>
- Owuor, S. O., Butterbach-bahl, K., Guzha, A. C., Rufino, M. C., Pelster, D. E., Díaz-Pinés, E., and Breuer, L. (2016). Groundwater recharge rates and surface runoff response to land use and land cover changes in semi-arid environments. *Ecological Processes*, 5(1), 1-21. <https://doi.org/10.1186/s13717-016-0060-6>
- Pinson S, Stollsteiner P. (2016). Typologie des bassins versants de la Bourgogne et modélisation hydrologique globale - Projet HYCCARE Bourgogne (Typology of Bourgone catchment areas and global hydrological modelling - HYCCARE Bourgogne Project). Rapport final BRGM/RP-65188- FR, 136 p., 76 ill., 2 Ann.
- Reiffsteck, P. (2003). Recommandations pour l'utilisation des géosynthétiques dans la lutte contre l'érosion (Recommendations for the use of geosynthetics in erosion control). Comité Français des Géosynthétiques. (128p).
- ROOSE, E. (1973). Dix-sept années de mesures expérimentales de l'érosion et du ruissellement sur un sol ferrallitique sableux de basse Côte d'Ivoire : contribution à l'étude de l'érosion hydrique en milieu intertropical (Seventeen years of experimental measurements of erosion and runoff on a sandy ferrallitic soil of the lower Ivory Coast: contribution to the study of water erosion in intertropical environments). Abidjan: Thèse Doct. Ing., Fac. Sci. Abidjan, Orstom, n° 20, 125 p.
- Shaban, A., Khawlie, M., and Abdallah, C. (2006). Use of remote sensing and GIS to determine recharge potential zones: the case of Occidental Lebanon. *Hydrogeology Journal*, 14(4), 433-443. <https://doi.org/10.1007/s10040-005-0437-6>
- Shaban, A. (2020): Water resources of Lebanon. Springer International Publishing. <https://doi.org/10.1007/978-3-030-48717-1>
- Singh, A., Panda, S. N., Kumar, K. S., and Sharma, C. S. (2013). Artificial groundwater recharge zones mapping using remote sensing and GIS: a case study in Indian Punjab. *Environmental Management*, 52(1), 61-71. <https://doi.org/10.1007/s00267-013-0101-1>
- Ta. M. Y., Lasm, T., Jourda, J. P, Saley, M. B., Miessan, G. A., Kouame, K. and Biemi, J. (2011). Cartographie des eaux souterraines en milieu fissuré par analyse multicritère. Cas de Bondoukou (Côte-d'Ivoire) (Groundwater mapping in fractured environments by multicriteria analysis. Case of Bondoukou (Côte-d'Ivoire)). *Revue Internationale de Géomatique*. 21, 43-71. <https://doi.org/10.3166/rig.21.43-71>
- Vasileva, T. (2019). An assessment of potential groundwater recharge zones in Bulgaria. *Geologica Balcanica*, 48/1, 43-61. <https://doi.org/10.52321/GeolBalc.48.1.43>
- Vila, J. M. (1994.a). Notice explicative de la carte géologique 1/50 000 de (265) (Explanatory note to the geological map 1/50 000 de (265)) : Edition du Service Géologique de l'Algérie, Boumerdes.
- Vila, J. M. (1994.b). Mise au point et données nouvelles sur les terrains triasiques des confins algéro-tunisiens : Trias Allochthon « glacier de sel » sous-marin et vrais diapirs (Development and new data on the Triassic terrains of the Algerian-Tunisian confines : Triassic Allochthon " salt glacier " underwater and real diapirs). *Mémoire du Service. Géologique de De l'Algérie* 7, 105-152.
- Vila, J. M. (1997). Carte géologique de AÏN TELIDJENE Feuille N° 265 échelle 1/50 000 (Geological map of AÏN TELIDJENE Sheet N° 265 scale 1/50 000).

Yao, T., Fouche-grobla, O., Oga, M. S., and Assoma, V. (2012). Extraction de linéaments structuraux à partir d'images satellitaires, et estimation des biais induits, en milieu de socle précambrien métamorphisé (Extraction of structural lineaments from satellite images, and estimation of induced biases, in a metamorphosed Precambrian basement environment. *Télé-détection*, 10/4, 161-178.

Zitouni, A., Boukdir, A., Mbaki, V. R. E., Baitie, W., Echakraoui, Z., El Fjiji, H., and Elissami, A. (2017). Contribution of the method of the electric resistivities in the gratitude (recongnition) of the aquifer turonien in the plain of Tadla and the tray of phosphates (Morocco). *Journal of Water Science and Environment Technologies*, 2(1).



This article is an Open Access article distributed under the terms and conditions of the Creative Commons Attribution 4.0 (CC BY 4.0) License (<http://creativecommons.org/licenses/by/4.0/>).